J. Electrochem. Sci. Eng. **16** (2026) 3446; https://doi.org/10.5599/jese.3446

Open Access : : ISSN 1847-9286
https://pub.iapchem.org/ojs/index.php/JESE

Original scientific paper

Highly sensitive and selective electrochemical determination of ciprofloxacin using modified screen-printed electrode

Hassan Ali M. Jawad

College of Pharmacy, Alfarahdi University, Baghdad, Iraq

Corresponding Author: assanalimohammed@uoalfarahidi.edu.iq

Received: May 8, 2026; Accepted: June 3, 2026; Published: July 8, 2026

Abstract

In this study, the Zn-based zeolitic imidazole framework-L (ZIF-L)/graphene oxide (ZIF-L(Zn)/GO) nanocomposite was prepared and used for ciprofloxacin detection. To detect ciprofloxacin (CFN), the nanocomposite was used to alter the screen-printed electrode' surface (ZIF-L(Zn)/GO/SPE). With a low limit of detection of 0.01 μM, good sensitivity of 0.1493 μA μM^{-1}, and a linear dependence between the current response and CFN concentration over the range of 0.05 to 300.0 μM, the sensor exhibited electro-catalytic behaviour toward CFN in phosphate buffer solution. Additionally, by identifying CFN in actual samples, the manufactured sensor's usefulness was shown.

Keywords

Antibiotic determination; voltametric sensor; modified electrode; graphene oxide composite; zeolitic imidazolate framework; antibiotics determination

Introduction

Water supplies have become contaminated during the past 30 years because people use pharmaceuticals more frequently. Here, antibiotics that resist degradation serve as permanent environmental hazards that endanger both human health and natural ecosystems [1]. Antibiotics have been one of the most problematic emerging pollutants because their chemical properties enable them to spread through various waste systems from hospitals, industries, and municipal areas, while they also create antibacterial resistance in microorganisms. The substances cause endocrine disruption and the development of antimicrobial resistance through their presence in aquatic environments at minimal concentrations, thereby destroying the natural life cycles of water-based ecosystems. Most antibiotics remain active for extended periods and are dangerous to living organisms, due to their non-biodegradable nature [2].

The main environmental pathways by which fluoroquinolone antibiotics, used primarily in medical treatments, enter the natural world involve their excretion in both urine and faeces [3]. Among these, ciprofloxacin (CFN), a medication that is frequently used to treat bacterial diseases

such as pneumonia and urinary tract infections, is effective against both Gram-positive and Gram-negative bacteria [4]. The World Water Organization has designated it as a priority medication of concern. The presence of CFN in even small quantities enables its biological accumulation in living organisms, which results in multiple dangerous impacts that include microflora toxicity, endocrine interruption and persistent toxic effects. The ecosystem and human health risks from CFN will decrease with effective removal methods, as its wastewater distribution creates dangerous environmental conditions at high concentrations due to its persistent nature and resistance to degradation, leading to eventual environmental contamination [5,6].

Antibiotics can be treated in the environment using a variety of techniques, including biological processes such as activated sludge and anaerobic digestion; physical processes such as membrane technologies and adsorption; chemical processes such as flocculation and coagulation; and hybrid methods such as advanced oxidation processes [7]. Although the chemical processes are quite simple to carry out, they may produce undesirable byproducts. Although biological methods are both operationally simple and economically viable, they often suffer from lengthy treatment times and insufficient antibiotic-removal efficiency. Physical approaches are more cost-effective and useful, but they need a large energy supply and periodic regeneration [8].

Analytical chemistry has undergone a dramatic change due to recent developments in electrochemical sensing, particularly the use of screen-printed electrodes (SPEs). SPEs have become an affordable and adaptable alternative to conventional electrochemical cells, which typically use bulk electrodes. Miniaturization, ease of use, customized electrochemical setups, and substantial cost savings, the cost per sensor has dropped from roughly 500 euros to as low as 1 euro, are some of the noteworthy advantages of using SPEs [9]. Reducing the required sample volume to only few microliters is another benefit of electrochemical sensor miniaturization. This helps to reduce the overall size of the diagnostic system and improves portability and ease of use in a variety of settings, including point-of-care (POC) applications [10,11].

Researchers are paying particular attention to metal-organic frameworks (MOFs) among micro- and nanocontainers because of their advantages, including controllable release performance, high inhibitor-loading capacity, large specific surface area, and adjustable pore structure [12]. These features make MOFs perfect for active corrosion protection. With well-organized pore architectures and tuneable chemical compositions, typical MOF particles are regular, crystalline porous materials composed of metal nodes and organic linkers. Inhibitors can be incorporated into MOF structures as organic ligands, and the environmental responsiveness of their framework connectivity ensures the material's intelligent corrosion prevention. A variety of MOFs, including Zn-based [14], Zr-based [15], and Fe-based MOFs, have been widely used to create intelligent anticorrosive coatings that enable self-healing in damaged areas. Although many studies have shown that MOFs can serve as nanoscale functional materials to enhance electrochemical sensor responses, the low electrical conductivity of MOF nanoparticles limits their electrochemical performance, rendering them inadequate for use in electrochemical sensors [17].

Preparing the composite based on MOFs is one efficient way to increase electrical conductivity. Large specific surface areas and high electrical conductivity make two-dimensional (2D) nanomaterials such as g-C_3N_4 and hexagonal boron nitride appealing platforms for building MOF-based composites. As a crucial 2D material, graphene oxide (GO) has several functional groups that facilitate effective chemical anchoring and integration with MOFs, and it exhibits strong congruence [20,21].

In this study, we developed a straightforward fabrication procedure for a voltammetric sensor based on ZIF-L(Zn)/GO. According to our research, ZIF-L(Zn)/GO/SPE demonstrated remarkable electrocatalytic activity in the oxidation of CFN. Excellent electrocatalytic activity, rapid response,

low detection limit, and high sensitivity were observed for the ZIF-L(Zn)/GO/SPE. Additionally, we assessed and used the ZIF-L(Zn)/GO/SPE sensor for CFN on actual samples.

Experimental

Reagent and apparatus

The analytical-grade reagents used in this experiment were manufactured by Merck and Sigma Aldrich. Phosphate buffer (PB) was used as the supporting electrolyte. The pH levels were adjusted using an aqueous sodium hydroxide solution. A pH meter (Metrohm 713) was used for pH measurements. An Autolab System PGSTAT302N (The Netherlands; EcoChemie) linked to a PC running GPES (version 4.9) data collection software was used to perform electrochemical measurements. SPEs (Dropsens, DRP 110) with graphite working and auxiliary electrodes and a silver pseudo-reference electrode were utilized.

Synthesis of ZIF-L (Zn)/GO nanocomposite

The ZIF-L (Zn)/GO nanocomposite was prepared by ultrasonically dispersing 30 mg of GO in 20 mL of deionized water for at least one hour to obtain a homogeneous solution. $Zn(NO_3)_2{\cdot}6H_2O$ (1 mmol or 0.297 g) was then added to the GO solution while being stirred. 2-methylimidazole (2-MI) (8 mmol or 0.655 g) was dissolved in 20 mL of deionized water to prepare an aqueous solution in a different beaker. The aqueous solution of 2-MI was gradually added to the suspension of GO and $Zn(NO_3)_2$ mentioned earlier, and the mixture was then ultrasonically dispersed for 10 minutes. The suspension was then magnetically agitated for two hours at room temperature. The precipitates were centrifuged multiple times to wash them with deionized water after the reaction period ended. The ZIF-L (Zn)/GO nanocomposite was produced after the precipitates were dried for 14 hours at 70 °C under vacuum.

Preparation of ZIF-L(Zn)/GO/SPE

A micropipette was used to deposit 3 µL of an aqueous nanocomposite suspension onto the working electrodes of the SPEs. 1 mg of nanocomposite and 1 mL of water were combined and ultrasonically stirred for forty minutes to create a homogeneous ZIF-L(Zn)/GO coating suspension. At room temperature, the resultant ZIF-L(Zn)/GO/SPE was dried.

Preparation of real samples

To prepare 0.1 M stock solutions (15 ml), the CFN tablets were thoroughly and evenly pulverized, sonicated for further dissolving, and filtered. Differential pulse voltammetry (DPV) was then performed by adding a transparent filtrate to 10 ml of 0.1 M PB at pH 7.0 in the electrochemical cell.

Additionally, 10 ml urine samples were centrifuged for 15 minutes at 2000 rpm. After passing through a 0.45 µm filter, a portion of the resulting supernatant was transferred into a 20 ml volumetric flask and diluted to volume with PB solution. The samples were then spiked with various CFN quantities. Finally, CFN concentrations were measured using the standard addition method.

Results and discussion

Electrochemical behaviours of CFN

Electrochemical oxidation of CFN at bare SPE and ZIF-L(Zn)/GO/SPE was compared by cyclic voltammetry (CV) (Figure 1). A small peak at about 1000 mV and with a current of 6.0 µA was found for CFN on the bare SPE (curve a), as shown in Figure 1. On the other hand, the CV of the modified electrode (curve b) showed an evaluated anodic peak at a less positive potential, suggesting

improved electrocatalytic oxidation of CFN. The oxidation current of CFN at the modified electrode increased by approximately 2.75-fold. These results suggest that the favourable properties of the nanocomposite are responsible for the increased electrooxidation of CFN at the modified electrode.

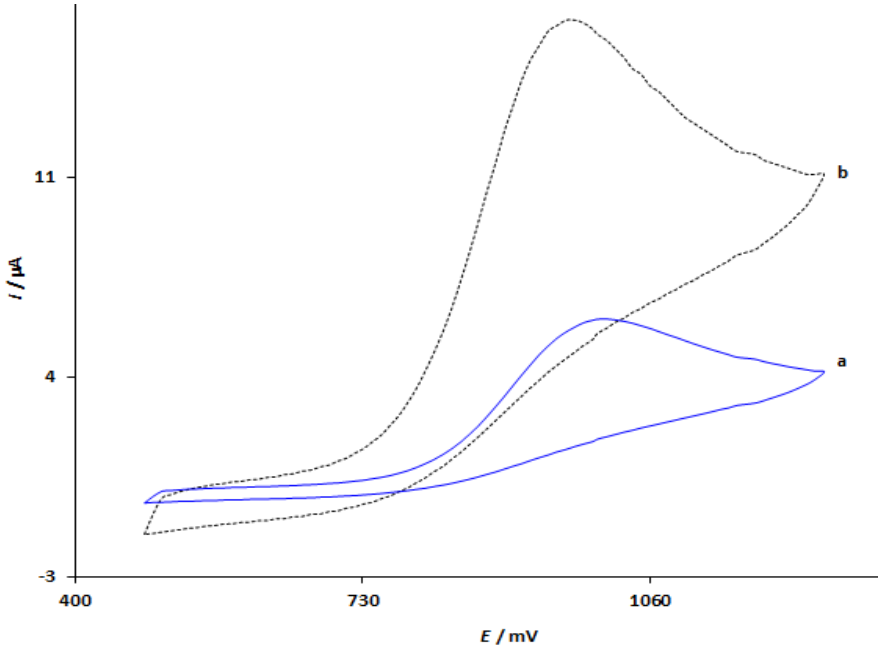

Figure 1. *CV responses of 100.0 µM CFN in PB 0.1 M (pH 7.0) at (a) bare SPE, and (b) ZIF-L(Zn)/GO/SPE. The scan rate is 50 mV* s^{-1}

Influence of scan rate on the electrooxidation of the CFN

Using ZIF-L(Zn)/GO/SPE, CV was performed over a range of scan rates to investigate the effect of scan rate (ν) on the peak current (I_p) (Figure 2). As can be seen, increasing the ν resulted in an increase I_p. I_{pa} and the $\nu^{1/2}$ for CFN oxidation were shown to have a linear relationship (inset). This implies that under these conditions, the oxidation of CFN at the modified electrode proceeds *via* diffusion control.

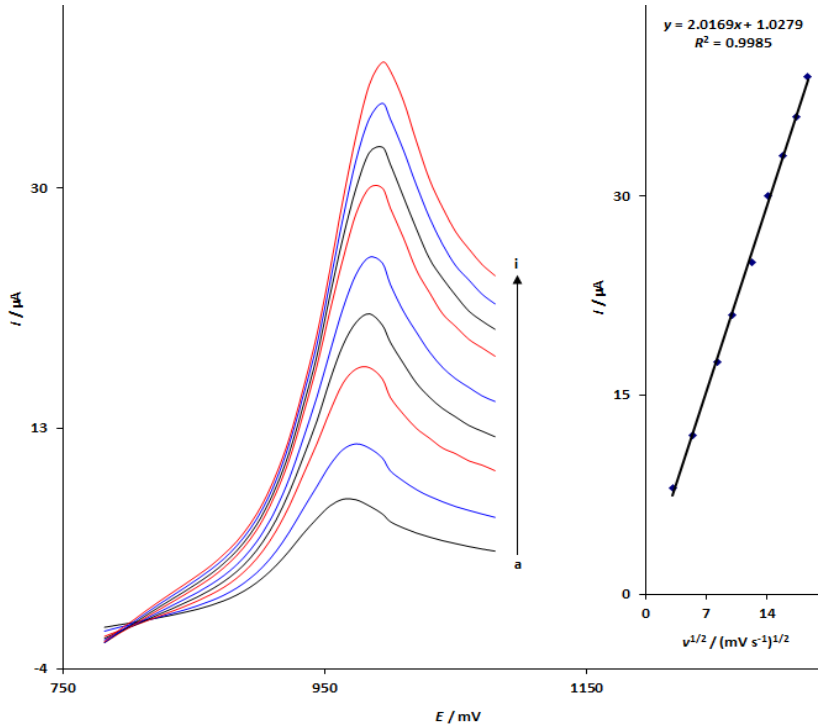

Figure 2. *CVs of modified electrode in 100.0 µM CFN in PBS (pH 7.0, 0.1 M) at different scan rates (a to I refer to 10, 30, 70, 100, 150, 200, 250, 300 and 350 mV* s^{-1}*. Inset: the variation of the* I_p vs. $\nu^{1/2}$

Chronoamperometric studies

The findings from chronoamperometric evaluations of different CFN concentrations conducted at the modified electrode are shown in Figure 3. The current of an electrochemical reaction with diffusion coefficient *D* is given by the Cottrell equation ($I = nFAC_bD^{1/2}\pi^{-1/2}t^{-1/2}$). The experimental data plots of *I* against $t^{-1/2}$ for different CFN concentrations and their matching best-fit curves were used (Inset A, Figure 3). The slopes of the derived linear equations were then plotted against the CFN levels (Inset B, Figure 3). The *D* parameter for CFN was obtained to be 1.5×10^{-5} cm^2 s^{-1}.

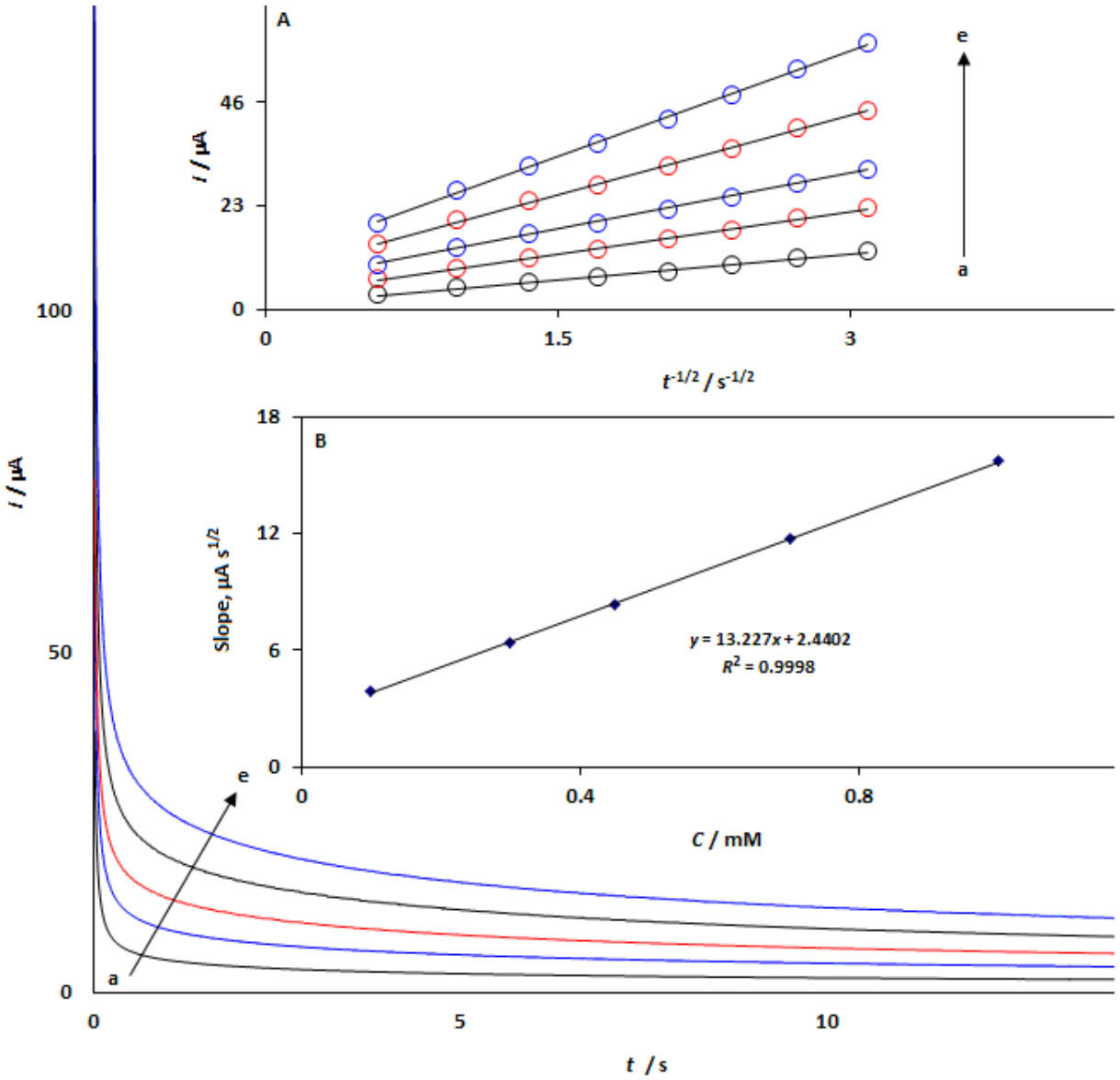

Figure 3. *Chronoamperograms for CFN at different concentrations (0.1, 0.3, 0.45, 0.7 and 1.0 mM) at ZIF-L(Zn)/ GO/SPE in 0.1 M PB (pH 7). Insets A)* I vs. $t^{-1/2}$ *linear graphs and Inset B) these lines' slopes against the* C_{CFN}

Analytical determination of CFN

Figure 4 shows the DPVs for CFN at various doses at ZIF-L(Zn)/GO/SPE in 0.1 M PBS (pH 7.0). An excellent linear relationship between CFN concentration and oxidation peak current was established over the range 0.05-300.0 µM under ideal conditions, as shown in the inset of Figure 4. The LOD for CFN was found to be 0.01 µM based on the experimental findings.

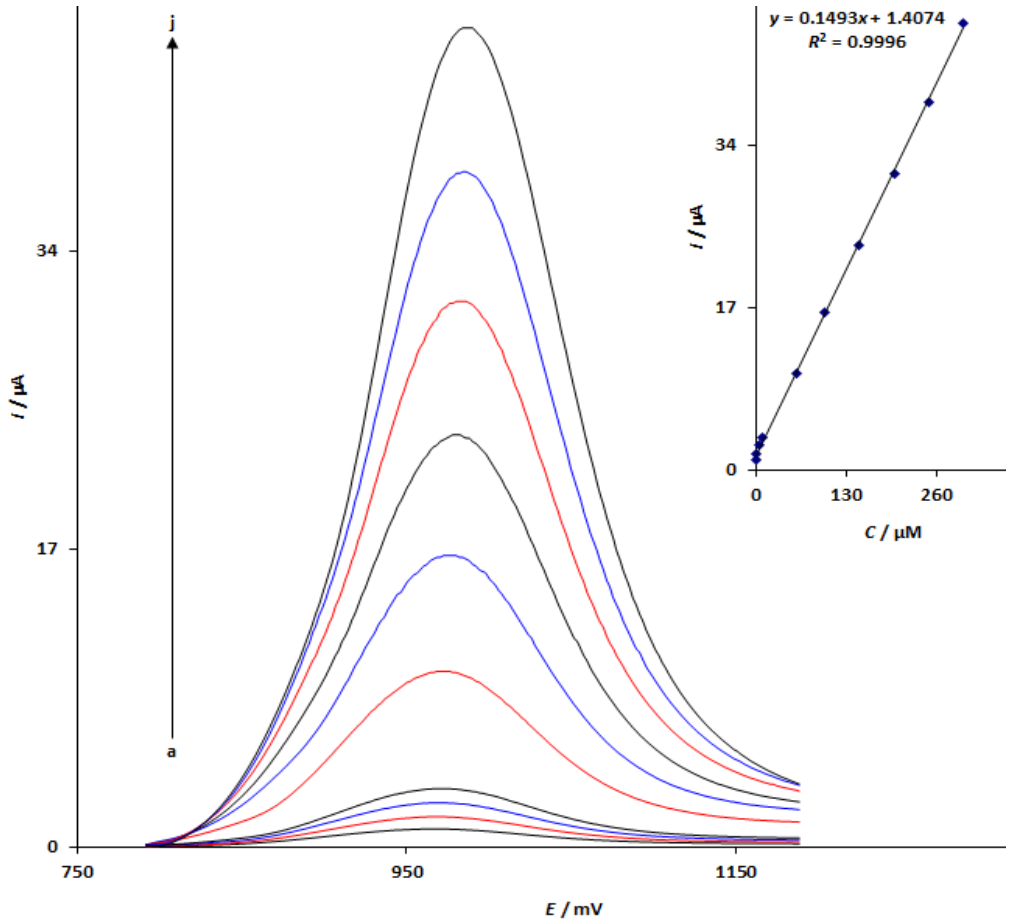

Figure 4. *DPVs of modified electrode in 0.1 M PB (pH 7) containing CFN (0.05, 1.0, 10.0, 60.0, 100.0, 150.0, 200.0, 250.0 and 300.0 µM). The plot of Ip versus the CFN concentrations (inset)*

Application of the analytical methodology to real samples

The manufactured electrode was used to measure CFN in human urine samples and CFN tablets to illustrate its practical use. For this reason, the conventional addition method was used. Table 1 displays the findings from the examination of actual specimens. Recoveries, ranging from 97.2 to 104.0 %, demonstrate the established method's efficacy and reliability in examining actual specimens.

Table 1. *Determination of CFN in real samples (n=5).*

Sample	Concentration, µM		Recovery, %	RSD, %
	Spiked	Found		
CFN tablet	0	3.1	-	3.5
	2.0	5.0	98.0	2.2
	3.0	6.3	103.3	2.9
	4.0	6.9	97.2	2.1
	5.0	8.2	101.2	2.7
Urine	5.0	5.2	104.0	2.4
	7.0	6.9	98.6	3.4
	9.0	8.8	97.8	1.9
	11.0	11.1	100.9	2.5

Conclusion

In conclusion, we have successfully created ZIF-L(Zn)/GO/SPE, an electrochemical sensor for CFN measurement. The electrochemical response of ZIF-L(Zn)/GO/SPE at a lower overpotential was

much higher for CFN than for bare SPE, as indicated by the CV studies. ZIF-L(Zn)/GO/SPE was used as a sensing platform to determine CFN, achieving ideal performance, including a low LOD of 0.01 µM and a wide linear response range (0.05 to 300.0 µM), owing to its effective oxidation of CFN. Lastly, the designed sensor's application was demonstrated by successful measurements of CFN in CFN tablets and urine samples, with good recovery values.

Funding: *Not applicable.*

References

[1] Z. Li, Z. Zhou, Y. Qin, D. Huang, M. Wang, Density functional theory assists in promoting advanced oxidation processes: Toward Efficient antibiotic degradation in waters, *Chinese Chemical Letters* **37** (2025) 112318. https://doi.org/10.1016/j.cclet.2025.112318

[2] X. O. Wei, Y. Zhao, Y. Ling, X. Chen, B. Liang, Y. Ben, C. B. Andrews, Z. Sun, C. Zheng, Advancing antibiotic detection in environmental waters: Standardization of solid phase extraction procedures and development of certified reference materials, *Sustainable Horizons* **15** (2025) 100153. https://doi.org/10.1016/j.horiz.2025.100153.

[3] P. Mathur, D. Sanyal, D. L. Callahan, X. A. Conlan, F. M. Pfeffer, Treatment technologies to mitigate the harmful effects of recalcitrant fluoroquinolone antibiotics on the environment and human health, *Environmental Pollution* **291** (2021) 118233. https://doi.org/10.1016/j.envpol.2021.118233.

[4] S. V. Zawar, S. Mahadik, Corneal deposit after topical ciprofloxacin as postoperative medication after cataract surgery, *Canadian Journal of Ophthalmology* **49** (2014) 392-394. https://doi.org/10.1016/j.jcjo.2014.04.013

[5] J. Tillonen, N. Homann, V. Salaspuro, M. Salaspuro, Ciprofloxacin medication decreases ethanol elimination rate in man, *Journal of Hepatology* **28** (1998) 132. https://doi.org/10.1016/S0168-8278(98)80720-4

[6] L. Yang, Z. Shen, N. Wu, B. Shi, R. Chen, Enhanced degradation of ciprofloxacin by α-Fe_2O_3@Sn-In_2S_3 composites with abundant vacancy via peroxymonosulfate activation, *Chemical Engineering Science* **333** (2026) 124198**.** https://doi.org/10.1016/j.ces.2026.124198

[7] Q. Feng, K. Guo, B. Liu, C. Wang, B. Yan, Q. Yue, Y. Gao, B. Gao, Recent advances and prospects in antibiotics removal by coagulation technique: A systematic review, *Journal of Cleaner Production* **514** (2025) 145825. https://doi.org/10.1016/j.jclepro.2025.145825

[8] G. You, H. Jin, M. Wu, Y. Li, X. You, C. Huang, Y. Xu, J. Hou, Insights into antibiotic resistance gene dynamics during Tanfloc-induced flocculation-storage process for cyanobacteria removal in an algae-laden drinking water source, *Journal of Environmental Management* **403** (2026) 129223. https://doi.org/10.1016/j.jenvman.2026.129223

[9] M. A. Azzam, A. Ahmad, A. A. Labib, W. A. Mohamed, A. K. El-Sawaf, H. T. Handal, Advanced Screen-Printed Electrodes: Shaping the Future of Electrochemical Wastewater Analysis, *Electrochimica Acta* **561**(2026) 148646. https://doi.org/10.1016/j.electacta.2026.148646.

[10] R. Muslim Muhibes, F. Khazaal, Q. M. Salih, R. Radi Karabat, Electrochemical determination of calcium folinate in the presence of methotrexate and 5-fluorouracil using UiO-66/CdS composite modified screen-printed carbon electrode, *ADMET and DMPK* **13** (2025) 2897. https://doi.org/10.5599/admet.2897

[11] S. Hong, S. Oh, E. Kim, E. Park, H. C. Chun, I. T. Kim, Y. R. Kim, Fabrication of screen-printed electrodes with long-term stability for voltammetric and potentiometric applications, *Sensors and Actuators Reports* **8** (2024) 100234. https://doi.org/10.1016/j.snr.2024.100234.

[12] R. K. Khundhur, Simultaneous determination of epinephrine and folic acid using MIL-101 (Fe)-NH_2 metal-organic framework/graphene oxide nanocomposite modified electrode, *ADMET and DMPK.* **13** (2025) 2762. https://doi.org/10.5599/admet.2762

[13] Y. Tao, K. Qi, Y. Qiu, X. Guo, Multifunctional MOF-based coating on magnesium enabling integrated properties of corrosion protection, biocompatibility and stimuli-responsive drug release, *Progress in Organic Coatings* **216** (2026) 110228. https://doi.org/10.1016/j.porgcoat.2026.110228.

[14] X. Bai, L. Hu, J. Xu, J. He, C. Deng, Y. Wu, A Stable Zn-MOF for Multifunctional Fluorescent Sensing of Fe^{3+} and Nitroaromatics, *Journal of Solid State Chemistry* **360** (2026) 126078. https://doi.org/10.1016/j.jssc.2026.126078.

[15] H. G. Abdel-Mohey, W. A. El-Mehalmey, M. A. Seleem, A. S. Mayhoub, H. I. Mohmed, W. I. El-Dougdoug, A. Baraka, M. H. Alkordi, Green synthesis of a water-stable thiol-decorated Zr-MOF for selective heavy metal removal, *RSC Sustainability* **4** (2026) 2264–2276. https://doi.org/10.1039/d5su00859j

[16] T. Su, L. Li, D. Liu, Q. Fan, Y. He, Y. Leng, Catalysis-enhanced colorimetric sensor array using Fe-MOF peroxidase mimetics for fingerprinting and discrimination of bisphenol species, *Microchemical Journal* **226** (2026) 118315**.** https://doi.org/10.1016/j.microc.2026.118315

[17] T. Dhanasekaran, P. S. Kumar, Y. K. Kim, B. Jeyaprabha, S. Lee, K. Kim, MOF and MXene-derived atom-level catalysts (Fe, co and Ni): Trends, breakthroughs, and challenges in water splitting, *Coordination Chemistry Reviews* **563** (2026) 218056. https://doi.org/10.1016/j.ccr.2026.218056

[18] A. Azeez, A. Bathinapatla, N. S. Bhujangaiah, Stable Layered Rod-like Cu-ADP MOF/g-C_3N_4 Photocatalyst for Visible-Light-Driven Chlorpyrifos Degradation and Biofunctional Applications, *Journal of the Indian Chemical Society* **103** (2026) 102649. https://doi.org/10.1016/j.jics.2026.102649

[19] X. Tian, S. Wang, W. W. Dong, J. Li, Y. Liu, J. Zhao, D. S. Li, In-situ anchoring of dye@ MOF on ultrathin boron nitride nanosheets (BNNS) for enhanced efficiency and stability, *Chemical Engineering Journal* **537** (2026) 176563**.** https://doi.org/10.1016/j.cej.2026.176563

[20] D. Wang, J. An, X. Chang, Y. Xu, J. Zhao, L. Gao, P. Zhang, X. Li, J. Nie, H. Cui, Autogenous-reduction-engineered MOF/GO hybrids as a universal ternary nanocomposite platform for simultaneous electrochemical sensing of uric acid, dopamine and ascorbic acid, *Electrochimica Acta* **562** (2026) 148711**.** https://doi.org/10.1016/j.electacta.2026.148711

[21] L. Fei, X. Ye, J. Yu, B. Chen, X. Zhu, Structural perfection through imperfection: Defect-engineered MOF-GO composite membrane for high-performance water purification, *Journal of Membrane Science* **749** (2026) 125404. https://doi.org/10.1016/j.memsci.2026.125404